ACS APPLIED MATERIALS & INTERFACES

Research Article

www.acsami.org

Surface Passivation Improves the Synthesis of Highly Stable and Specific DNA-Functionalized Gold Nanoparticles with Variable DNA Density

Jashmini Deka,[†] Rostislav Měch,[‡] Luca Ianeselli,[†] Heinz Amenitsch,[§] Fernando Cacho-Nerin,[§,∥] Pietro Parisse,[⊥] and Loredana Casalis*[,†,⊥]

[†]Elettra-Sincrotrone Trieste, s.s. 14 km 163.5 in Area Science Park, 34149 Basovizza, Trieste Italy

[‡]Institute of Physical Engineering, Brno University of Technology, Technická 2, 61669 Brno, Czech Republic

[§]Institute for Inorganic Chemistry, Graz University of Technology, Stremayrgasse 9/V, A-8010 Graz, Austria

[∥]Diamond Light Source Ltd, Diamond House, Harwell Science and Innovation Campus, OX11 0DE Didcot, United Kingdom

[⊥]INSTM − ST Unit, s.s. 14 km 163.5 in Area Science Park, 34149 Basovizza, Trieste Italy

Supporting Information

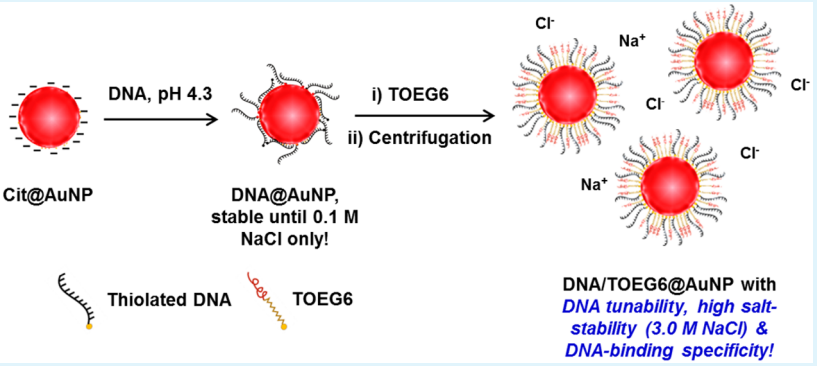

ABSTRACT: We report a novel and multifaceted approach for the quick synthesis of highly stable single-stranded DNA (ssDNA) functionalized gold nanoparticles (AuNPs). The method is based on the combined effect of surface passivation by (1-mercaptoundec-11-yl)hexa(ethylene glycol) and low pH conditions, does not require any salt pretreatment or high excess of ssDNA, and can be generalized for oligonucleotides of any length or base sequence. The synthesized ssDNA-coated AuNPs conjugates are stable at salt concentrations as high as 3.0 M, and also functional and specific toward DNA−DNA hybridization, as shown from UV−vis spectrophotometry, scanning electron microscopy, gel electrophoresis, fluorescence, and small angle X-ray scattering based analyses. The method is highly flexible and shows an additional advantage of creating ssDNA-AuNP conjugates with a predefined number of ssDNA strands per particle. Its simplicity and tenability make it widely applicable to diverse biosensing applications involving ssDNA functionalized AuNPs.

KEYWORDS: *DNA functionalization, gold nanoparticles, surface passivation, oligo ethylene glycol, salt-stability, specificity, variable DNA density*

INTRODUCTION

Gold nanoparticles (AuNPs) show unique (size and/or shape dependent) electrical, catalytic, thermal, and optical properties arising from the collective behavior of the electrons confined at the nanoscale, making them a promising candidate for application in the field of nanotechnology in general and nanobiotechnology in particular.[1,2] Moreover, the ease of functionalization of AuNPs by promoting self-assembly of simple or complex (generally thiolated or aminated) molecules on its surface is an added advantage. On the other hand, single-stranded DNA (ssDNA) finds a vast application in both biological[3] as well as nonbiological[4−7] fields such as sensing, photonics, optoelectronics, and structural nanotechnology, because of the unique specificity of DNA−DNA hybridization. Not surprisingly, a great number of works have been recently reported based on the use of ssDNA-AuNPs conjugates (DNA@AuNPs), because of the great potential of their combined effects.[8−11] In this framework, many efforts are directed toward easy and quick methods to functionalize AuNPs with ssDNA, retaining DNA functionality and specificity.

Received: February 11, 2015
Accepted: March 10, 2015
Published: March 10, 2015

DOI: 10.1021/acsami.5b01191
ACS Appl. Mater. Interfaces 2015, 7, 7033−7040

Scheme 1. Formation of High Salt Stable DNA/TOEG6@AuNPs[a]

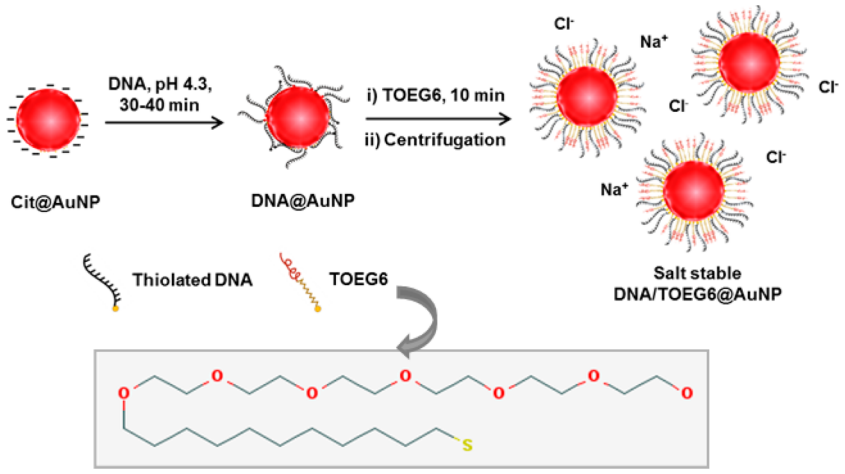

[a]Chemical structure of TOEG6 has been shown below the scheme.

Citrate-stabilized gold nanoparticles (cit@AuNPs), synthesized by the reduction of Au^{3+}, are most commonly used for the synthesis of DNA@AuNPs.[12] However, the electrostatic repulsion between the negatively charged AuNPs and the phosphate backbones of the ssDNA molecules, constitutes the limiting step during ssDNA functionalization of cit@AuNPs. To overcome this drawback, salt-aging recipes have been extensively employed to screen the negative charges and bring ssDNA strands and particles closer for interaction.[13,14] However, these methods require stepwise addition of salt and are time-consuming. A large body of recent literature reports emphasized shortening the synthesis time.[15−20] Articles on other related aspects of the synthesis of DNA@AuNPs, such as the role of AuNP radius on ssDNA loading,[21] maximization of ssDNA loading,[22] and functionalization kinetics[23] are also increasing. Most of these works deal with the use of surfactants in addition to the saline buffer or with some pretreatment of the AuNPs before ssDNA functionalization to make the salt-aging faster,[22] to enhance salt-stability of the DNA@AuNPs, and/or to allow the use of high salt conditions,[18] required for subsequent ssDNA-biomolecules interaction. Surfactants in these cases are either used in the reaction buffer[18] or are coating the NPs[17,20] prior to the addition of ssDNA. Recently, synthesis at low pH has been introduced as an alternative to salt-aging methods to reduce synthesis time, based on the principle that at low pH the overall surface charge density and thus the repulsion between particles and ssDNA is reduced, thereby facilitating the interaction between the negatively charged ssDNA and AuNPs.[24] However, this low pH method was optimized for 13 nm cit@AuNPs and could not be generalized for AuNPs of all sizes. Zhang et al. further reported that for larger AuNPs, a large excess of ssDNA was required to apply the low pH method and obtain stable conjugates.[23] For example, 10X excess of the theoretical ssDNA loading capacity was required to synthesize stable conjugates with 20 nm AuNPs as compared to 1.5× of ssDNA excess used for 13 nm AuNPs.

In this manuscript, we present a novel and flexible approach, for the quick synthesis of AuNPs functionalized with tunable density of ssDNA. The method neither requires any salt pretreatment nor a high-excess of ssDNA, and the particles show remarkable stability at high salt concentration (up to 3.0 M NaCl) and high specificity toward DNA-binding. The novelty of the approach lies in the use of low pH conditions (to make the process faster), along with the use of a mixed self-assembled monolayer (SAM) of thiolated ssDNA and of a protein-repellent alkanethiol, to entirely passivate the AuNP surface, thus providing stability to the particles against salt induced aggregation. This method also allows for tuning the number of ssDNA on the NP surface which is desirable for applications where controllable DNA based nanoassembly of AuNPs plays a significant role.[25,26] To the best of our knowledge, this is the first time that a method has been proposed based on the principle of cochemisorption on the surface of AuNPs, to achieve highly stable particles without any prerequisite of salt or surfactants.

RESULTS AND DISCUSSION

SAMs of thiolated ssDNA with variable density are being produced on flat Au surface for various applications. Such monolayers are often post-treated with PEG-terminated alkanethiols to exchange with the nonspecifically and weakly bound ssDNA molecules through their nitrogen-bases or phosphate groups.[27,28] This process also promotes surface hydrophilicity and resistance to nonspecific interactions with matrix proteins.[29] In analogy to flat surfaces, top-terminated oligo (ethylene glycol) alkanethiol, (1-mercaptoundec-11-yl)hexa(ethylene glycol) referred to as TOEG6 throughout this paper (see Scheme 1), was chosen to promote the formation of a mixed monolayer on AuNPs, based on the expertise of our research group on SAM formation on flat Au surfaces.[30−32] AuNPs capped with TOEG6-only SAMs have been previously reported to be kinetically stable and soluble in the presence of moderate concentration of monovalent and divalent metal salts.[33] A few works have been reported so far, which focus on the synthesis of mixed SAMs of ssDNA and alkanethiols on AuNP surfaces, to achieve salt-stable DNA@AuNPs.[34−36] However, salt pretreatment or complicated steps were employed to obtain stable DNA@AuNP particles rendering the methods time-consuming.

In the present work, TOEG6 was introduced to cit@AuNPs (approximately 20 nm in size) after a short incubation period with the ssDNA at pH 4.3. The AuNPs thereby covered with ssDNA and TOEG6 were separated from the rest of the unbound molecules by centrifugation and washing steps (for details refer to Experimental Section). The procedure takes a total of 50 min and involves very simple steps. The time of

DOI: 10.1021/acsami.5b01191
ACS Appl. Mater. Interfaces 2015, 7, 7033−7040

incubation and the concentration of TOEG6 had to be optimized to prevent the replacement of all the ssDNA strands by TOEG6. For our work, we used a ssDNA:AuNP ratio equal to 300 (which is 1.5X of the theoretical capacity of ssDNA loading on 20 nm AuNP).[23] The post-treatment of DNA@AuNPs with TOEG6 results in AuNPs with a mixed monolayer (DNA/TOEG6@AuNPs) which were found to be highly stable. The stepwise formation of stable DNA/TOEG6@AuNPs is summarized in Scheme 1.

The diameter of the cit@AuNPs used was found to be (17 ± 2) nm from small-angle scattering X-ray (SAXS) analysis and (19 ± 2) nm from scanning electron microscopy (SEM) analysis, respectively. The small difference between the particle sizes obtained from the two methods may be due to the fact that two different batches of cit@AuNPs were used for each analysis. The model fit to the SAXS data considered Schultz distributed sticky hard spheres (see Figure S1 in the Supporting Information, SI for details). The successful functionalization of ssDNA on the NPs was confirmed by gel electrophoresis of DNA/TOEG6@AuNPs using DNA@AuNPs and cit@AuNPs as controls (Figure 1). Because it was possible to track the

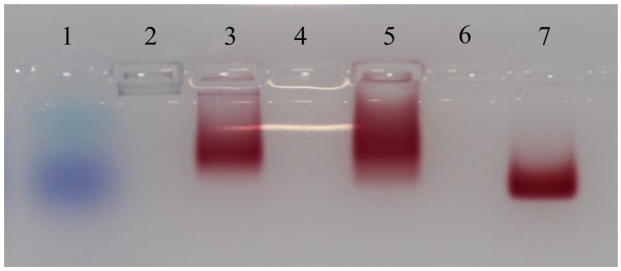

Figure 1. Electrophoresis gel image of DNA/TOEG6@AuNPs, DNA@AuNPs, and cit@AuNPs only. Lane 1 was loaded with ssDNA loading dye, Lane 2 with cit@AuNPs, Lane 3 with DNA1/TOEG6@AuNPs, Lane 5 with DNA2/TOEG6@AuNPs, and Lane 7 with DNA1@AuNPs.

movement of the NPs along the gel due to their color, no dye was used for NP loading. However, for reference, the ssDNA loading dye (which is normally used to load ssDNA on the gel) was placed in lane 1. The cit@AuNPs did not move at all (lane 2) and tended to aggregate in the well turning from red to purple. Instead, the movement of DNA1@AuNPs, DNA1/TOEG6@AuNP, and DNA2/TOEG6@AuNP could be observed even with naked eyes (lane 7, lane 3, and lane 5, respectively), which is a clear sign of the presence of ssDNA on the NPs. DNA1/TOEG6@AuNP or DNA2/TOEG6@AuNP moved less than the DNA1@AuNPs along the gel, confirming the reduced number of ssDNA strands on these particles with respect to the DNA1@AuNPs as a result of the partial replacement of ssDNA with neutral TOEG6. Sequences of DNA 1 and DNA2 are shown in Table 1.

The total number of ssDNA strands loaded on a NP following this protocol was quantified by means of a procedure based on a 6-FAM (carboxyfluorescein) tagged ssDNA (DNA-F) with the same base sequence as DNA2. The assay details and calibration graph are included in the Experimental Section and Figure S2 in the Supporting Information, respectively. It was found that 41 ssDNA strands were attached to each NP. Hill et al. and Zhang et al. have reported a total of about 200 strands of ssDNA being attached to a 20 nm AuNP by following the low pH and salt aging method, respectively.[21,23]

Table 1. Base Sequences of the Various ssDNAs Used Throughout the Work[a]

ssDNA nomenclature	base sequence
DNA1	5′-gtt gcc ata aaa-3′-SH
DNA2	5′-agt cgt tta aaa-3′-SH
DNA1(long)	5′-gtt gcc att ttt ttt ttt tt-3′-SH
DNA2(long)	5′-agt cgt ttt ttt ttt ttt tt-3′-SH
DNA3	3′-atg cct ata atc tgt tcc gtt ttt ttt ttt-5′-SH
DNA4	3′-acg gaa cag att ata ggc att ttt ttt ttt-5′-SH
DNA5	3′-ttt ttt ttt ttt cag aag cag gag cat ggg cta caa aag cgt ttt ttt ttt ttt tt-5′-SH
DNA6	3′-ttt ttt ttt ttt cgc ttt tgt agc cca tgc tcc tgc ttc tgt ttt ttt ttt ttt tt-5′-SH
Dup-DNA1	5′-atg gca act ata cgc gct ag-3′
Dup-DNA2	5′-aaa cga ctc tag cgc gta ta-3′
DNA-F	6-FAM-5′-agt cgt tta aaa-3′-SH

[a]DNA1 and DNA2 were thiol C3 modified at the 3′ end; DNA1 (long) and DNA2 (long) were thiol C6 modified at the 3′ end; DNA3, DNA4, DNA5, and DNA6 were thiol C6 modified at the 5′ end; DNA-F was modified with the fluorophore 6-FAM at the 5′ end and thiol C3 modified at the 3′ end. They were purchased from biomers.net.

Because our approach made use of TOEG6, which replaces some of the ssDNA strands, it is reasonable that our AuNP would have a reduced number of ssDNAs loaded on it. A discrete number of DNA molecules per particle can be exploited for constructing DNA/AuNPs based novel functional architectures for biosensing applications.[25]

The particles were further tested for their stability at high salt concentration, which is a favorable condition for DNA hybridization. Surface plasmon resonance (SPR) peaks of DNA1/TOEG6@AuNPs were analyzed at increasing concentrations of salt. Figure 2A shows the UV−vis spectra of DNA1/TOEG6@AuNPs at 0 and 3.0 M salt concentrations. The narrow band of the SPR peak of the NPs with the maximum at 522 nm suggests the presence of particles with a narrow size distribution range similar to the unmodified cit@AuNPs. Interestingly no change in the shape of the spectrum was seen even at 3.0 M NaCl, suggesting no change in the state of the AuNPs and confirming the high stability of the particles. On the other hand, the particles coated with DNA1 only (DNA1@AuNPs) were found to be stable only up to 0.1 M of NaCl concentration as indicated from the SPR spectra (Figure 2B). At 0.4 M of NaCl concentration, the SPR peak of DNA1@AuNPs broadened with a second peak appearing at 676 nm, suggesting aggregation of the AuNPs at salt concentrations higher than 0.1 M.

Results similar to DNA1/TOEG6@AuNPs have been obtained for DNA2 and longer ssDNA strands (20, 30, and 56 bases long respectively; see Table 1 and Figure S3 in the Supporting Information), indicating that the method is generally applicable. The higher salt tolerance of ssDNA coated AuNPs in the presence of TOEG6 as compared to AuNPs coated with ssDNA only, proven by UV−vis spectrophotometry analysis, can be related to the absence of noncovalently and weakly bound ssDNA strands, lying horizontally on the AuNP surface.[37]

To further prove the salt-stability of DNA1/TOEG6@AuNPs, we also performed SAXS-based analyses at various concentrations of salt, up to 1.0 M. For these measurements commercially available 20 nm cit@AuNPs were used (Sigma-

DOI: 10.1021/acsami.5b01191
ACS Appl. Mater. Interfaces 2015, 7, 7033−7040

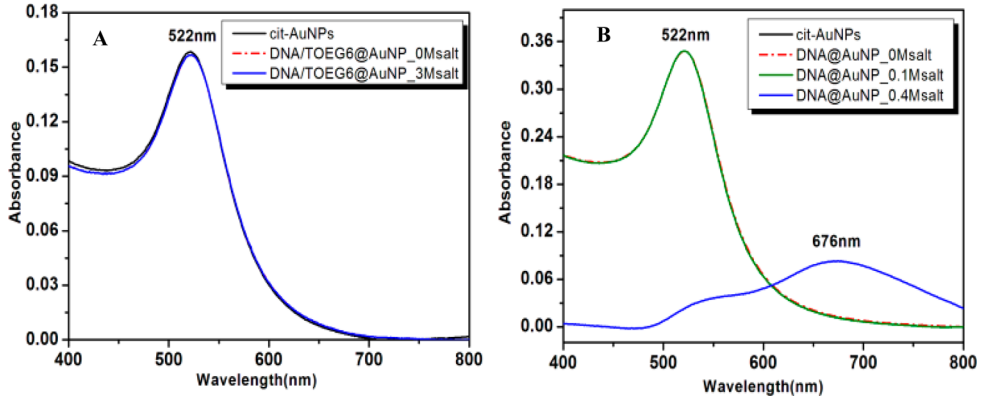

Figure 2. UV−vis spectra (SPR peaks) of (A) DNA1/TOEG6@AuNPs and (B) DNA1@AuNPs at various NaCl concentrations.

Aldrich Chemical Co.). The monodispersity of these particles was slightly higher than those produced in our lab, which made the commercial version more suitable for SAXS measurements. Analysis of the SAXS data reveals monodisperse particles with a size of (20 ± 2) nm (Figure 3) in good agreement with the

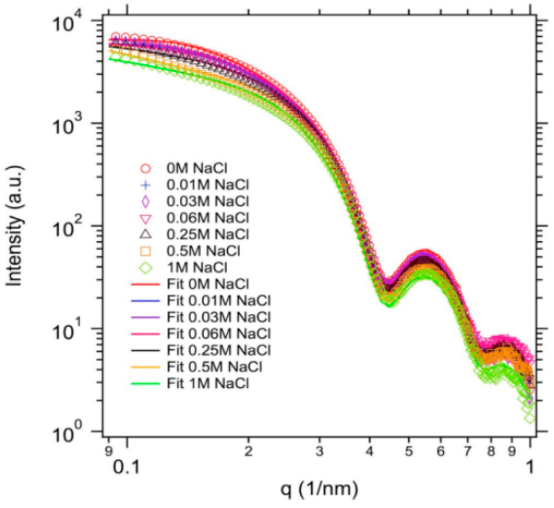

Figure 3. SAXS patterns of DNA1/TOEG6@AuNPs at various concentrations of NaCl and their respective fits using the form factors of the sphere with Schultz distribution as their size distribution and a hard sphere model for the structure factor.

specifications. The results did not reveal appreciable changes as a function of the salt concentration indicating very little or no interaction among the functionalized AuNPs even at 1.0 M NaCl concentration, which confirms their stability (see Experimental Section for more details and Table S1 in the Supporting Information for the full fit results).

Reports in the literature suggest that the strength of nucleobase interaction with the AuNP surface increases in the order of $T < C < A < G$ making ssDNAs with some bases more susceptible than others to lie down on the AuNP surface nonspecifically (and therefore making the NPs less stable).[38] In our case, the presence of TOEG6 in the mixed SAM makes the particles immune to these base-sequence induced stability issues, making our approach general for all kinds of ssDNAs irrespective of the base-sequence. We have obtained stable NPs with ssDNAs containing poly A base sequence (A4, in DNA1 and DNA2, see Table 1) close to the thiol group linked to the AuNP surface, proving that our method overcomes the instabilities associated with the base-sequence.

To check the functionality of our DNA/TOEG6@AuNPs, we mixed two different batches of DNA/TOEG6@AuNP conjugates (made of DNA1 and DNA2 respectively) together, at 1.0 M salt concentration. Following the work of C.A. Mirkin et al.,[13,14] a duplex solution (dup-DNA1 plus dup-DNA2) with partially complementary strands to DNA1 and DNA2 respectively was added to the mixture and left at room temperature (refer to Table 1 for the ssDNA sequences). Within a few minutes the color of the solution turned from red to purple and larger aggregates settled down within a few hours, suggesting that the hybridization between the complementary ssDNAs led to the formation of 3D networks of the NPs (as shown schematically in Figure 4A). In the absence of the duplex strands, however, the mixture of two batches remained red, indicating the absence of nonspecific binding between particles functionalized with different, noncomplementary ssDNAs (see Section S4 of the Supporting Information for additional tests on the specificity of DNA/TOEG6@AuNPs). Time dependent UV−vis spectra were also acquired to follow the changes in the SPR peak upon addition of the duplex solution which initiates hybridization. The control shows no change in the SPR peak shape indicating no reaction among the two batches of AuNPs (Figure 4B), whereas the solution with the duplex showed prominent peak shift and broadening with time (Figure 4C), due to the AuNP aggregation resulting from of DNA−DNA linking through the duplex. Figure 4D, E shows SEM images of the mixture of the two batches of AuNPs in the absence and presence of duplex after 3 h, respectively, after drop-casting on a bare Au substrate. The photograph of the respective samples has been shown in insets. The SEM image and the color of the mixture clearly indicate aggregation of the NPs only in the presence of the duplex, further confirming that the ssDNAs tagged on the AuNPs by our approach were functional.

In the present method, the post-treatment of DNA@AuNPs with TOEG6 replaces the loosely bound ssDNAs on the NP surface and produces stable ssDNA-coated AuNPs. Because the replacement of the ssDNAs is based on the competition between the alkanethiol chains of the ssDNA (3 or 6 −CH2 units) and TOEG6 (11 −CH2 units) to stably bind to the NP surface, it is quite likely that even the ssDNA strands chemisorbed to the NP surface through their thiol groups might be prone to replacement by the TOEG6 molecules if the DNA@AuNPs are exposed for a longer time or to higher concentrations of TOEG6. We wanted to check whether this

DOI: 10.1021/acsami.5b01191
ACS Appl. Mater. Interfaces 2015, 7, 7033−7040

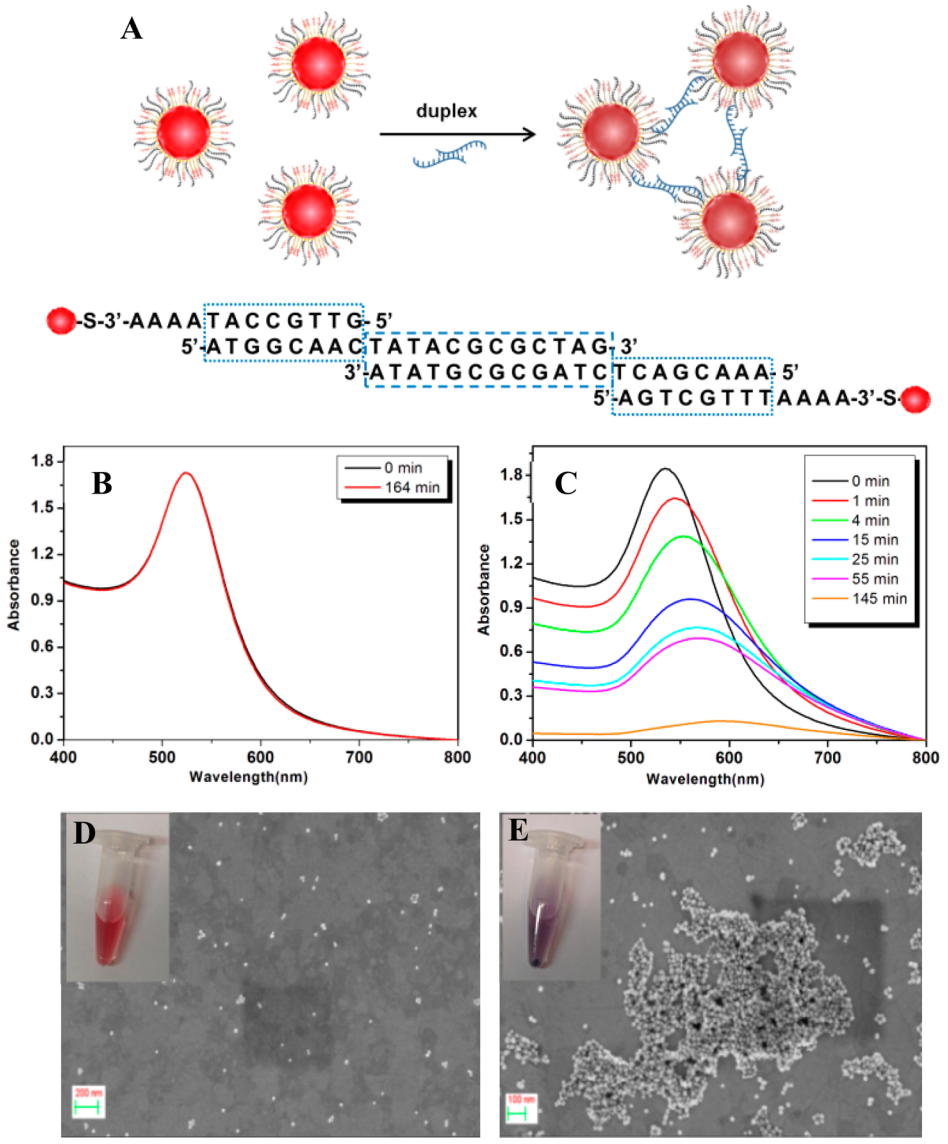

Figure 4. (A) Schematics showing nanoparticles forming aggregates when the duplex is introduced to the mixture of two batches of nanoparticles with DNA1 and DNA2, respectively. The duplex is partially complementary to DNA1 and DNA2 and the formation of the aggregates is caused by the hybridization of duplex with both sticky ends with DNA1 and DNA2 (as shown under the scheme); UV−vis spectra of the mixture of DNA1/TOEG6@AuNPs and DNA2/TOEG6@AuNPs (B) absence and (C) presence of the duplex as a function of time; SEM images of the mixture in the (D) absence and (E) presence of the duplex after 3 h, being dropcasted on a bare Au substrate. The insets show the picture of the respective samples. The scale bars are 200 and 100 nm, respectively.

characteristic could be used to tune the amount of ssDNAs on the NP surface. Toward this goal, we post-treated the DNA@AuNPs with five different concentrations of TOEG6 (2.7, 3.3, 4.0, 6.0, and 8.0 μM) following the same protocol as in the previous experiments with 2.0 μM of TOEG6. The total number of ssDNA strands loaded on a NP in each case was quantified by means of the fluorescence based procedure described above. The numbers of ssDNA strands attached per NP are summarized in Table 2. As expected, the higher the TOEG6 concentration, the fewer were ssDNA strands per NP, demonstrating that our method can be exploited to tune the amount of ssDNA on the NP surface. Previously, a similar approach based on the competitive binding of a small molecule (oligo ethylene glycol, OEG), with ssDNA has been reported to manipulate ssDNA surface density on AuNPs.[39] However, that method involved pretreating the AuNPs with mononucleotide and using salt along with the OEG molecule to achieve the same purpose.

Table 2. Number of ssDNA Attached per NP in the DNA/TOEG6@AuNP Particles Corresponding to Various Concentrations of TOEG6, Keeping the Rest of the Protocol Unchanged[a]

[AuNP] (nM)	[DNA] (μM)	[TOEG6] (μM)	no. of ssDNAs/NP
0.8	0.232	2.0	**41**
0.8	0.232	2.7	**36**
0.8	0.232	3.3	**24**
0.8	0.232	4.0	**10**
0.8	0.232	6.0	**7**
0.8	0.232	8.0	**6**

[a]Refer to the Experimental Section for details of the quantification method.

DOI: 10.1021/acsami.5b01191
ACS Appl. Mater. Interfaces 2015, 7, 7033−7040

The DNA/TOEG6@AuNPs with different amounts of ssDNA thus produced were analyzed for their salt-stability and ssDNA-functionality. For the salt-stability, SPR peaks of DNA1/TOEG6@AuNPs were recorded at increasing concentrations of salt. In all cases, the SPR spectrum presents a single narrow band peaking at 522 nm, with no change in the shape of the spectrum even at a salt concentration of 3.0 M, which suggests that the AuNPs remain unchanged and confirms the high stability of the particles for all the ratios of ssDNA:TOEG6 investigated so far (see Figure S5 in the Supporting Information).

The DNA functionality was also tested for all ssDNA densities using the same method explained above. In all cases except the two with the lowest ssDNA surface density (7 and 6 ssDNA/NP), the SPR peak broadened with time, indicating conjugate hybridization and therefore preservation of the ssDNA-functionality (see Figure S6 in the Supporting Information). Thus, we conclude that a minimum of 10 ssDNAs per NP seems to be the necessary condition to achieve functional DNA/TOEG6@AuNPs.

CONCLUSIONS

We have presented a novel approach that combines low pH with the concept of alkanethiol (TOEG6)-DNA mixed SAMs formation, to achieve highly stable ssDNA functionalized AuNPs with high salt tolerance, in a short time. The method proposed is advantageous over other existing methods that either involve several hours of synthesis time, complicated pretreatment steps of the NPs, use of toxic surfactants or depend on the presence of salt.[13−21] The introduction of an alkanethiol to the ssDNA monolayer on AuNP was found to be a better alternative to the use of a large excess of ssDNA to achieve more radially stretched ssDNA strands on the NP surface to maintain stability in the presence of salt. In addition to bringing salt-stability, the mixed monolayer of TOEG6 and ssDNA allows the preservation of ssDNA functionality, enhances the resistance to nonspecific binding as well as specificity in DNA−DNA hybridization process with respect to particles functionalized with ssDNA only. The method is also independent of the nucleobase sequence and length of the ssDNA being attached to the NP. Such properties make our nanoparticles suitable for application in biological samples (ssDNA/RNA sensing, enzymatic assays of ssDNA or drug delivery systems) where pH, salt concentration, and nonspecific interactions can often hinder the targeting of the desired molecules. Moreover, changing the TOEG6 concentration and/or exposure time, provides the possibility to modulate the number of ssDNA strands attached per NP and still retain all the functionality and stability. Because of its simplicity, flexibility, generality, and the ability to address multiple issues, the method presented here should be useful in a wide range of applications; from biosensing to controlled design of DNA/AuNP based nanoarchitectures.

EXPERIMENTAL SECTION

Preparation of Citrate-Stabilized AuNPs (cit@AuNPs). cit@AuNPs were prepared by a known method of citrate reduction of $HAuCl_4$.[12] 1.095 mL of 1.73×10^{-2} M $HAuCl_4$ (Sigma-Aldrich Chemical Co.) was added to 43.605 mL of Milli-Q grade water and brought to boil. Then 300.0 μL of 72.0 mg/mL trisodium citrate 2-hydrate (Merck) was added at once to the boiling solution and the boiling (or refluxing) was continued for another 30 min to ensure complete reduction of $HAuCl_4$. The solution turned from colorless to deep red, indicating the synthesis of AuNPs. The red solution was removed from the heat and allowed to cool at room temperature. The AuNPs were used as prepared for the experiments.

Synthesis of DNA@AuNPs. ssDNA (5.22 μL of 100 μM) was added to 750.0 μL of AuNPs mixed by vortexing and left to rest for 10 min. After this, the pH of the medium was adjusted to 4.3 by an addition of 1.5 mL of 4.3 pH citrate-HCl buffer. The mixture of ssDNA and AuNPs was incubated at room temperature for another 30 min. The solution was centrifuged at 14 000 rpm for 10 min and the supernatant was discarded to remove the unbound ssDNA from the functionalized AuNPs. The pellet was resuspended and centrifuged washed twice with Milli-Q water, at the speed of 14 000 rpm for 10 min each. The final pellet was redispersed in 1.0 mL of 10 mM phosphate buffer (pH 7.0).

Synthesis of DNA/TOEG6@AuNP. ssDNA (5.22 μL of 100 μM) was added to 750.0 μL of AuNPs mixed by vortexing and left for 10 min. After this, the pH of the medium was brought to 4.3 by an addition of 1.5 mL of citrate-HCl buffer of pH 4.3. The mixture of ssDNA and AuNPs was incubated at room temperature for another 30 min after which 15.0 μL of 300.0 μM (1-mercaptoundec-11-yl)hexa(ethylene glycol) (TOEG6) (Sigma-Aldrich Chemical Co.) was added. The mixture was then vortexed well and left to rest for another 10 min. The solution was centrifuged at a speed of 14 000 rpm for 10 min and the supernatant was discarded to remove the unbound ssDNA and TOEG6 molecules from the functionalized AuNPs. The pellet was resuspended and centrifuged twice in Milli-Q water, washed twice at 14 000 rpm for 10 min each time. The final pellet was redispersed in 1.0 mL of 10 mM phosphate buffer (pH 7.0).

Salt Stability Test of DNA/TOEG6@AuNP. Various combinations of 3.5 M NaCl and DNA/TOEG6@AuNP were vortex mixed so as to have 0 to 3.0 M of salt concentration in a final volume of 100 μL solution. The solutions were incubated for about 1 h and then analyzed spectrophotometrically (Lambda 25 UV/vis spectrometer, PerkinElmer). The solutions were scanned between 400 and 800 nm. Before each scan the instrument was set to autozero by performing the baseline correction with a phosphate buffer saline of corresponding concentration of the NaCl. Separate plastic cuvettes were used for each measurement.

Gel Electrophoresis. DNA1/TOEG6@AuNP, DNA2/TOEG6@AuNP, DNA1@AuNP, and cit@AuNPs pellets were collected after two washes, mixed with 10% glycerol and loaded onto a 1% agarose gel, run at 30 V. Since the AuNPs are colored and their movement could be traced in the gel, there was no need to mix a ssDNA-dye with them. However, as a reference of the molecule movement in the gel conditions, ssDNA-dye was loaded in lane 1of the gel.

Quantification of ssDNA Loaded on DNA/TOEG6@AuNP. To determine the number of ssDNA strands attached to the DNA/TOEG6@AuNP, we attached a fluorescent ssDNA (DNA-F, with the same base sequence as DNA2) to AuNPs following the same procedure as for DNA/TOEG6@AuNP. The DNA-F/TOEG6@AuNP thus prepared was redispersed in 0.2 M phosphate buffer, pH 8.0. The DNA-F was displaced from the DNA-F/TOEG6@AuNP by adding equal volumes of DNA-F/TOEG6@AuNP and 1.0 M DTT in 0.2 M phosphate buffer, pH 8.0. An overnight incubation of the mixture ensures the complete displacement of DNA-F from the AuNPs. The AuNPs were then separated from the solution by centrifugation at 14,000 rpm for 10 min. The supernatant collected was checked for fluorescence using a luminescence spectrometer (Infinite 200Pro, TECAN), exciting at 485 nm and collecting emission at 535 nm. To convert the fluorescence reading from the solution to DNA-F concentration, we generated a calibration curve with known concentrations of DNA-F prepared in the same DTT buffer solution and analyzed in the same well plate (Figure S2 in the Supporting Information).

SAXS Analysis. DNA1/TOEG6@AuNP was prepared as mentioned above, but using commercially available 20 nm sized AuNPs as purchased (Sigma-Aldrich Chemical Co.). DNA1/TOEG6@AuNP was mixed with different amounts of NaCl to obtain final salt concentrations of 0.01, 0.03, 0.06, 0.25, 0.50, and 1.0 M, respectively. SAXS patterns were acquired at the Austrian SAXS beamline[40] at

DOI: 10.1021/acsami.5b01191
ACS Appl. Mater. Interfaces 2015, 7, 7033−7040

synchrotron radiation facility Elettra−Sincrotrone Trieste. Data were collected using an imaging plate (Mar300, Mar Research GmbH, Germany) covering a spatial range $q = 0.08-1\ nm^{-1}$, with $q = (4\pi \sin\theta)/\lambda$, where 2θ is the scattering angle and λ the photon wavelength (1.54 Å in our case). The same glass capillary (Ø 1.5 mm) was used to measure all samples, and for each sample, the corresponding buffer with the same salt concentration was measured as the background. As a control DNA1/TOEG6@AuNP was tested with no salt. The temperature was set to 25 °C.

The data were processed with the Fit2D program[41] and subsequently analyzed with Igor Pro (v. 6.3, Wavemetrics Inc., USA) using custom routines. In particular, the scattering profiles were fit to a model that considers the nanoparticles to interact and have variable size. The number distribution of the sizes was approximated by the Schulz distribution, while the interaction, i.e., the structure factor, was assumed to follow a sticky hard sphere model.[42]

To Check the Specificity of DNA−DNA Binding in the Conjugates. An Au substrate was dipped in a mixture of DNA2 and TOEG6 (in the ratio of 1:100) in TE buffer, pH 8.0, and left to incubate overnight to obtain a mixed SAM of DNA2/TOEG6. Following this, the substrate was washed with water and dried in a N_2 stream. Separately, a duplex solution was prepared by heating a mixture of dup-DNA1 and dup-DNA2 in phosphate buffer, pH 7.0 and 1.0 M NaCl at 50 °C for 15 min followed by annealing. Thirty μL of this solution was drop-casted on the substrate with the mixed SAM and left to incubate overnight. After washing and drying, 30 μL of DNA1/TOEG6@AuNP in the presence of 1.0 M NaCl was drop-casted and incubated overnight, followed by washing and drying. As a control, the same treatment was done on another Au substrate skipping the addition of the duplex. As a second control, DNA1@AuNP was used instead of DNA1/TOEG6@AuNP on the DNA2/TOEG6 mixed SAM on Au substrate without the duplex solution. Dup-DNA1 and dup-DNA2 are partially complementary to DNA1 and DNA2 respectively; hence the duplex can act as a linker between the Au substrate and DNA1/TOEG6@AuNPs. The resulting substrates were analyzed for the presence of AuNPs by Scanning Electron Microscopy (Zeiss Supra-40). Details are discussed in Section S4 in the Supporting Information.

Tuning and Quantification of the ssDNA Amount on AuNPs. DNA-F/TOEG6@AuNPs were prepared for analysis as explained above. To tune the amount of DNA-F attached to the NP, the volume of TOEG6 added was changed from 15.0 to 20.0, 25.0, 30.0, 45.0, and 60.0 μL of 300 μM for preparing five different batches of DNA/TOEG6@AuNPs. The supernatant obtained in each case after DTT treatment was analyzed to calculate the amount of DNA-F attached. Fifty microliters of the respective solutions were loaded in triplicates into a 96 well plate. The samples were analyzed by luminescence spectrometry using the same method explained above. For comparison a regular batch with 15.0 μL was also prepared under the same conditions. Fluorescence intensity was converted into DNA-F concentration using the same calibration curve as before.

■ ASSOCIATED CONTENT

Supporting Information

Specificity tests and relative SEM images; UV−vis spectra of AuNPs functionalized with various ssDNAs and of AuNPs functionalized with different DNA/AuNP ratios; UV−vis spectra for salt stability and ssDNA functionality tests for AuNPs with SAM of different ssDNA/TOEG6 ratios; SAXS results; fluorescence calibration for DNA quantification on the particles. This material is available free of charge via the Internet at http://pubs.acs.org.

■ AUTHOR INFORMATION

Corresponding Author

*E-mail: loredana.casalis@elettra.trieste.it.

Author Contributions

The manuscript was written through contributions of all authors. All authors have given approval to the final version of the manuscript.

Funding

This work was supported by a FIRB 2011 grant "Nanotechnological approaches toward tumor theragnostic" (P.P. and L.C.), and FIRB 2011 grant "Nano-solar: Photocatalytic Nanosystems for artificial photosynthesis and hydrogen production by solar-driven water splitting" (J.D.)

Notes

The authors declare no competing financial interest.

■ ACKNOWLEDGMENTS

The authors are grateful to Prof. Lucia Pasquato and Dr. Paolo Pengo for useful discussions, Mr. Aditya Mojumdar, Dr. Alessandro Bosco, and Miss Maryse Nkoua for kindly helping with the gel−electrophoretic and SAXS experiments.

■ REFERENCES

(1) Daniel, M. C.; Astruc, D. Gold Nanoparticles: Assembly, Supramolecular Chemistry, Quantum-size-related Properties, and Applications Toward Biology, Catalysis, and Nanotechnology. *Chem. Rev.* **2004**, *104*, 293−346.

(2) De, M.; Ghosh, P. S.; Rotello, V. M. Applications of Nanoparticles in Biology. *Adv. Mater.* **2008**, *20*, 4225−4241.

(3) Drummond, T. G.; Hill, M. G.; Barton, J. K. Electrochemical DNA Sensors. *Nat. Biotechnol.* **2003**, *21*, 1192−1199.

(4) Pinheiro, A. V.; Han, D.; Shih, W. M.; Yan, H. Challenges and Opportunities for Structural DNA Nanotechnology. *Nat. Nanotechnol.* **2011**, *6*, 763−772.

(5) Kwon, Y. W.; Lee, C. H.; Choi, D. H.; Ji, J. I. Materials Science of DNA. *J. Mater. Chem.* **2009**, *19*, 1353−1380.

(6) Slinker, J. D.; Muren, N. B.; Renfrew, S. E.; Barton, J. K. DNA Charge Transport Over 34 nm. *Nat. Chem.* **2011**, *3*, 228−233.

(7) Aldaye, F. A.; Sleiman, H. F. Dynamic DNA Templates for Discrete Gold Nanoparticle Assemblies: Control of Geometry, Modularity, Write/Erase and Structural Switching. *J. Am. Chem. Soc.* **2007**, *129*, 4130−4131.

(8) Lin, Y. W.; Liu, C. W.; Chang, H. T. DNA Functionalized Gold Nanoparticles for Bioanalysis. *Anal. Methods* **2009**, *1*, 14−24.

(9) Carrara, S. Nano-Bio-Technology and Sensing Chips: New Systems for Detection in Personalized Therapies and Cell Biology. *Sensors* **2010**, *10*, 526−543.

(10) Zanoli, L. M.; Agata, R. D.; Spoto, G. Functionalized Gold Nanoparticles for Ultrasensitive DNA Detection. *Anal. Bioanal. Chem.* **2012**, *402*, 1759−1771.

(11) DeLong, R. K.; Reynolds, C. M.; Malcolm, Y.; Schaeffer, A.; Severs, T.; Wanekaya, A. Functionalized Gold Nanoparticles for the Binding, Stabilization, and Delivery of Therapeutic DNA, RNA, and other Biological Macromolecules. *Nanotechnol. Sci. Appl.* **2010**, *3*, 53−63.

(12) Frens, G. Controlled Nucleation for the Regulation of the Particle Size in Monodisperse Gold Suspensions. *Nat. Phys. Sci.* **1973**, *241*, 20−22.

(13) Storhoff, J. J.; Elghanian, R.; Mucic, R. C.; Mirkin, C. A.; Letsinger, R. L. One-Pot Colorimetric Differentiation of Polynucleotides with Single Base Imperfections Using Gold Nanoparticle Probes. *J. Am. Chem. Soc.* **1998**, *120*, 1959−1964.

(14) Elghanian, R.; Storhoff, J. J.; Mucic, R. C.; Letsinger, R. L.; Mirkin, C. A. Selective Colorimetric Detection of Polynucleotides Based on the Distance-Dependent Optical Properties of Gold Nanoparticles. *Science* **1997**, *277*, 1078−1081.

(15) Zhao, W.; Lin, L.; Hsing, I.-M. Rapid Synthesis of DNA-Functionalized Gold Nanoparticles in Salt Solution Using Mono-

DOI: 10.1021/acsami.5b01191
ACS Appl. Mater. Interfaces 2015, 7, 7033−7040

nucleotide-Mediated Conjugation. *Bioconjugate Chem.* **2009**, *20*, 1218−1222.
(16) Gill, R.; Goeken, K.; Subramaniama, V. Fast, Single-Step, and Surfactant-Free Oligonucleotide Modification of Gold Nanoparticles Using DNA with a Positively Charged Tail. *Chem. Commun.* **2013**, *49*, 11400−11402.
(17) Xu, V.; Yuan, H.; Xu, A.; Wang, J.; Wu, L. Rapid Synthesis of Stable and Functional Conjugates of DNA/Gold Nanoparticles Mediated by Tween 80. *Langmuir* **2011**, *27*, 13629−13634.
(18) Zhang, X.; Servos, M. R.; Liu, J. Ultrahigh Nanoparticle Stability against Salt, pH, and Solvent with Retained Surface Accessibility via Depletion Stabilization. *J. Am. Chem. Soc.* **2012**, *134*, 9910−9913.
(19) Yang, H.; Heng, X.; Hu, J. Salt- and pH-Resistant Gold Nanoparticles Decorated with Mixed-Charge Zwitterionic Ligands, and Their pH-Induced Concentration Behavior. *RSC Adv.* **2012**, *2*, 12648−12651.
(20) Zu, Y.; Gao, Z. Facile and Controllable Loading of Single-Stranded DNA on Gold Nanoparticles. *Anal. Chem.* **2009**, *81*, 8523−8528.
(21) Hill, H. D.; Millstone, J. E.; Banholzer, M. J.; Mirkin, C. A. The Role Radius of Curvature Plays in Thiolated Oligonucleotide Loading on Gold Nanoparticles. *ACS Nano* **2009**, *3*, 418−424.
(22) Hurst, S. J.; Jean, K. R. L.; Mirkin, C. A. Maximizing DNA Loading on a Range of Gold Nanoparticle Size. *Anal. Chem.* **2006**, *78*, 8313−8318.
(23) Zhang, X.; Gouriye, T.; Goeken, K.; Servos, M. R.; Gill, R.; Liu, J. Toward Fast and Quantitative Modification of Large Gold Nanoparticles by Thiolated DNA: Scaling of Nanoscale Forces, Kinetics, and the Need for Thiol Reduction. *J. Phys. Chem. C* **2013**, *117*, 15677−15684.
(24) Zhang, X.; Servos, M. R.; Liu, J. Instantaneous and Quantitative Functionalization of Gold Nanoparticles with Thiolated DNA Using a pH-Assisted and Surfactant-Free Route. *J. Am. Chem. Soc.* **2012**, *134*, 7266−7269.
(25) Zhang, T.; Yang, Z.; Liu, D. DNA Discrete Modified Gold Nanoparticles. *Nanoscale* **2011**, *3*, 4015−1421.
(26) Loweth, C. J.; Caldwell, W. B.; Peng, X. G.; Alivisatos, A. P.; Schultz, P. G. DNA-Based Assembly of Gold Nanocrystals. *Angew. Chem., Int. Ed.* **1999**, *38*, 1808−1812.
(27) Herne, T. M.; Tarlov, M. J. Characterization of DNA Probes Immobilized on Gold Surfaces. *J. Am. Chem. Soc.* **1997**, *119*, 8916−8920.
(28) Boozer, C.; Ladd, J.; Chen, S.; Yu, Q.; Homola, J.; Jiang, S. DNA Directed Protein Immobilization on Mixed ssDNA/Oligo(ethylene glycol) Self-Assembled Monolayers for Sensitive Biosensors. *Anal. Chem.* **2004**, *76*, 6967−6972.
(29) Schollbach, M.; Zhang, F.; Roosen-Runge, F.; Skoda, M. W.; Jacobs, R. M.; Schreiber, F. Gold Nanoparticles Decorated with Oligo(Ethylene Glycol) Thiols: Surface Charges and Interactions with Proteins in Solution. *J. Colloid Interface Sci.* **2014**, *426*, 31−38.
(30) Castronovo, M.; Lucesoli, A.; Parisse, P.; Kurnikova, A.; Malhotra, A.; Grassi, M.; Grassi, G.; Scaggiante, B.; Casalis, L.; Scoles, G. Two-Dimensional Enzyme Diffusion in Laterally Confined DNA Monolayers. *Nat. Commun.* **2011**, *2*, 1−10.
(31) Parisse, P.; Vindigni, A.; Scoles, G.; Casalis, L. In Vitro Enzyme Comparative Kinetics: Unwinding of Surface-Bound DNA Nanostructures by RecQ and RecQ1. *J. Phys. Chem. Lett.* **2012**, *3*, 3532−3537.
(32) Corvaglia, S.; Sanavio, B.; Enriquez, R. P. H.; Sorce, B.; Bosco, A.; Scaini, D.; Sabella, S.; Pompa, P. P.; Scoles, G.; Casalis, L. Atomic Force Microscopy Based Nanoassay: A New Method to Study α-Synuclein-Dopamine Bioaffinity Interactions. *Sci. Rep.* **2014**, *4*, 5366.
(33) Aryal, B. P. *Protein-nanoparticle Conjugates: Developing Biosensors for Small Molecule Detection*. Ph.D. Thesis, Wayne State University, Detroit, MI, 2008.
(34) Jans, H.; Stakenborg, T.; Jans, K.; Van de Broek, B.; Peeters, S.; Bonroy, K.; Lagae, L.; Borghs, G.; Maes, G. Increased Stability of Mercapto Alkane Functionalized Au Nanoparticles Towards DNA Sensing. *Nanotechnology* **2010**, *21*, 1−8.
(35) Stakenborg, T.; Peeters, S.; Reekmans, G.; Laureyn, W.; Jans, H.; Borghs, G.; Imberechts, H. Increasing the Stability of DNA-Functionalized Gold Nanoparticles Using Mercaptoalkanes. *J. Nanopart. Res.* **2008**, *10*, 143−152.
(36) Claridge, S. A.; Liang, H. W.; Basu, S. R.; Frechet, J. M. J.; Alivisatos, A. P. Isolation of Discrete Nanoparticle−DNA Conjugates for Plasmonic Applications. *Nano Lett.* **2008**, *8*, 1202−1206.
(37) Zhao, W.; Lee, T. M. H.; Leung, S. S. Y.; Hsing, I.-M. Tunable Stabilization of Gold Nanoparticles in Aqueous Solutions by Mononucleotides. *Langmuir* **2007**, *23*, 7143−7147.
(38) Demers, L. M.; Ostblom, M.; Zhang, H.; Jang, N.-K.; Liedberg, B.; Mirkin, C. A. Thermal Desorption Behavior and Binding Properties of DNA Bases and Nucleosides on Gold. *J. Am. Chem. Soc.* **2002**, *124*, 11248−11249.
(39) Zhao, W.; Hsing, I.-M. Facile and Rapid Manipulation of DNA Surface Density on Gold Nanoparticles Using Mononucleotide-Mediated Conjugation. *Chem. Commun.* **2010**, *46*, 1314−1316.
(40) Amenitsch, H.; Rappolt, M.; Kriechbaum, M.; Mio, H.; Laggner, P.; Bernstorff, S. First Performance Assessment of the Small-Angle X-ray Scattering Beamline at ELETTRA. *J. Synchrotron Radiat.* **1998**, *5*, 506−508.
(41) Hammersley, A. P.; Svensson, S. O.; Hanfland, M.; Fitch, A. N.; Häusermann, D. Two Dimensional Detector Software: From Real Detector to Idealised Image or Two-Theta Scan. *High Pressure Res.* **1996**, *14*, 235−248.
(42) Pontoni, D.; Finet, S.; Narayanan, T.; Rennie, A. R. Interactions and Kinetic Arrest in an Adhesive Hard-Sphere Colloidal System. *J. Chem. Phys.* **2003**, *119*, 6157−6165.

DOI: 10.1021/acsami.5b01191
ACS Appl. Mater. Interfaces 2015, 7, 7033−7040